TEMPERATURE RISE IN INDUCTION MOTOR WINDINGS AS THE CAUSE OF VARIATION IN ROTATIONAL SPEED OF AN AXIAL FAN

by

Živan T. SPASIĆ[a*], Milan M. RADIĆ[b], and Dragana G. DIMITRIJEVIĆ[a]

[a] Faculty of Mechanical Engineering, University of Nis, Nis, Serbia
[b] Faculty of Electronic Engineering, University of Nis, Nis, Serbia

Original scientific paper
DOI: 10.2298/TSCI16S5449S

The paper presents results of an experimental investigation performed under controlled laboratory conditions, in order to identify real causes of variation in the rotational speed of an axial fan that can be noticed after a certain period following the start of operation. The theoretical background important for understanding the observed phenomenon is given and the hypothesis is proposed which states that the temperature rise in motor windings and a consequential rise of their resistances are responsible for such specific behavior of the axial fan. The experiment was performed on a standard test rig with a small industrial axial fan, driven by a three-phase induction motor with the rated power of 1.5 kW. The experimental procedure is described in details, measured and calculated results are presented and appropriate conclusions are given. The obtained experimental results confirm the proposed hypothesis.

Key words: *axial fan, induction motor, temperature rise, speed variation*

Introduction

Three-phase induction motors are the main source of mechanical power used today in industrial processes of different types. There are estimations claiming that approximately 55% percent of the total energy delivered to the industry worldwide is actually consumed by three-phase induction motors [1]. Proved reliability, robustness, low production and maintenance costs are main reasons for widespread usage of this type of motor. Traditionally, induction motors were considered as machines with poor regulation characteristics, and they were predominantly used for drives that required almost constant rotational speed, with small variations from no-load to full load operation. In the close future, an even greater expansion of the application of induction motors can be expected, due to significant advances in manufacturing of power electronic devices, whose primary function is the control of rotational speed and delivered mechanical torque.

Most of industrial and public utility systems intended for the transport of fluids are usually powered by three-phase induction motors. The application of power electronic devices for regulation of rotational speed is usually avoided, unless it is necessary in order to achieve the exact efficient operating point. Axial fans are very often used for obtaining a forced flow

* Corresponding author; e-mail: zivans@masfak.ni.ac.rs

of a gas in different types of processes, and if carefully engineered and coupled with appropriate induction motor, they can operate with relatively high efficiency, even with unregulated speed. The most common assumption is that, if the geometry of a fan impeller and a suction duck is constant, the system will operate in a stationary regime, characterized by a constant rotational speed.

From the theory of axial fans, it is known that gained mass flow and pressure depend on rotational speed by the linear and square law, respectively [2]. If a certain type of very sensitive process has to be supplied by a forced gas flow from an axial fan, a possible variation in rotational speed has to be taken into consideration. For example, small variations in speed can usually be caused by variable voltage in the electric grid. However, the detailed testing of a reversible axial fan, performed in the laboratory, showed that even with constant voltage applied to the induction motor, rotational speed of the axial fan is not constant, and shows tendency of slight decrease soon after the start of operation, as reported in [3].

The hypothetical explanation of the observed phenomenon was also offered in [3], but no experimental proof was given. In this paper, we go one step further and present new experimental results, so as to confirm a previously established hypothesis, that the temperature rise in induction motor windings has an inevitable consequence, shown through a small reduction of rotational speed in the steady state operation, compared to the speed observed immediately after the start of operation. It is important to mention that a different type of axial fan impeller has been used in this investigation, which is the reason why the obtained experimental results are different from the ones presented in [3].

Theoretical background

The stationary operating point of a system consisting of an axial fan and a mechanically coupled induction motor is defined by the intersection of torque-speed curves that analytically describe both parts of the system. As for the axial fan, the torque-speed curve shows complex dependency of mechanical torque demanded for the operation with the arbitrary value of rotational speed, and it is usually obtained experimentally [2]. In the region characterized by low volumetric flows, the behavior of the axial fan is quite unpredictable, and that region is considered an unstable operating area. However, in the normal operating region, mechanical torque demanded from the fan shaft can be described by the exact mathematical function, dependent on the value of rotation speed n [rpm], *i. e.* $M_{\text{fan}} = \text{f}(n)$, where the exact analytical expression depends on the actual construction of the fan (*i. e.* the number of blades and the shape of blade profiles), and also on the density of the transported gas.

From the theory of induction machines [1, 4], it is known that electromagnetic torque developed by a three-phase induction motor is defined:

$$M_{\text{mot}} = \frac{3}{\Omega'}\frac{R_1''}{s}\frac{U_f^2}{\left(R' + \nu'\frac{R_1''}{s}\right)^2 + (X_\gamma' + \nu' X_{\gamma k1}'')^2} \tag{1}$$

If all parameters of the equivalent circuit (fig. 1) influencing the value of the developed electromagnetic torque are considered as constant (except the actual rotational speed, n), the unique functional dependence $M_{\text{mot}} = \text{f}(n)$ can be calculated. Neglecting the rotational losses in an induction machine (*i. e.* friction and ventilation of machine itself), we can further say that the available shaft torque is equal to the developed electromagnetic torque. Thus, a

unique operating point could be defined in the intersection of the two torque characteristics, and the system would have to rotate at fixed speed.

However, the previous consideration is far from reality, since all of parameters describing an induction machine have a variable nature. In normal operating regimes, some of them can be indeed considered as constant, without concerns that the accuracy of the analysis will be lost. Such an assumption is valid for reactances X'_γ, $X''_{\gamma k1}$, and X_m, and also for the resistance R_m in the magnetization branch of the circuit, if the applied phase voltage and frequency have constant values (U_f = const. and f = const.). On the contrary, stator and rotor resistances R' and R_1'' are highly dependent on the actual temperature of the windings, according to the relation:

$$R_{T2} = R_{T1}\frac{T_2 - 38}{T_1 - 38} \tag{2}$$

if conductors are made of copper, or to the relation:

$$R_{T2} = R_{T1}\frac{T_2 - 18}{T_1 - 18} \tag{3}$$

if conductors are made of aluminum [1].

In eqs. (2) and (3), R_{T1} [Ω] represents the resistance of the winding at the temperature T_1 [K], and R_{T2} [Ω] represents the resistance of the winding at the temperature T_2 [K].

An induction motor can be represented by its equivalent circuit, shown in fig. 1. The main difference that can be noticed, compared to the standard equivalent circuit, is that stator and rotor resistances R' and R_1'' are considered as variable elements, whose values depend on the actual temperature of the winding, T.

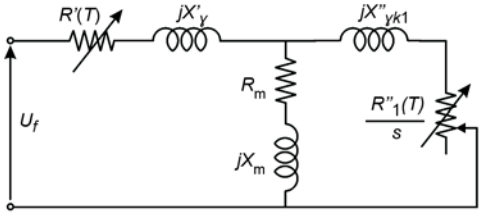

Figure 1. Equivalent circuit of an induction motor with variable stator and rotor resistances

Depending on the type of material used for insulation of the induction machine windings during the production process, induction motors are classified into six different thermal tolerance classes, Y, A, E, B, F, and H, according to [5]. Contemporary induction motors are usually produced in the F thermal tolerance class, which allows a rise in the mean windings temperature of ΔT = 105 K above the standardized ambient temperature $T_{\mathrm{a\,nom}}$ = 313 K, and also includes a *reserve* of additional rise of ΔT_{hs} = 10 K for *hot spots* in the winding. This information has to be understood properly, and it should be clear that, although the mentioned standard allows maximum absolute allowable temperature in the hot spots of the winding $T_{\mathrm{max\,hs}}$ = 428 K , maximum allowable *mean temperature of the winding* (which is, in fact, obtained by calculations, according to detected rise in resistance of a winding) has to be limited to T_{max} = 418 K. Using eqs. (2) and (3), and having in mind that the stator windings are made of copper wire, while the rotor cage is made of aluminum, the stator winding resistance can achieve values that are approximately 50% higher compared with the resistances at the supposed ambient temperature of T_a = 293 K.

Such an increase in temperature of the induction motor windings will inevitably lead to the rise of winding resistances, and according to eq. (1), will further cause significant deviations of the induction motor torque-speed curve. For the sake of better understanding the pre-

sented phenomenon, a typical deformation of induction motor torque-speed curves, caused by an increased resistance in windings is shown in fig. 2. The solid line represents the torque-speed curve of the motor calculated with resistances R'_a and R''_{1a}, valid for the supposed ambient temperature of T_a = 293 K, while the dash-dot line represents the same type of curve, but calculated with *hot* resistances R'_h and R''_{1h} at the mean temperature of the winding T_{max} = 418 K, and actually being 50% higher compared with the values of R'_a and R''_{1a}. Plotted curves have an illustrative purpose only, and were calculated using a set of equivalent electric circuit parameters typical for a four-poles, low-voltage induction motor with the rated power of P_n = 1.5 kW and with a single rotor cage.

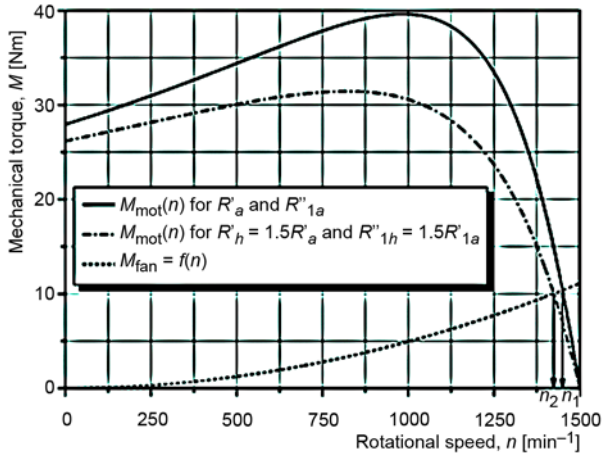

Figure 2. Theoretical drift of operating point caused by increased resistances of motor windings

The segment of the fan torque-speed curve, significant for this analysis (in the region of normal operation), is plotted with the dotted line in fig. 2. It is obvious that with increased resistances of the induction machine windings, the intersection of torque-speed curves is expected to migrate from the higher value n_1 to a somewhat lower value of rotational speed, n_2. A decrease in rotational speed $\Delta n = n_1 - n_2$ in the presented theoretical example is about 30 min^{-1} or 2% of the machine synchronous speed n' = 1500 min^{-1}, but it should be mentioned that during the normal operation of a properly chosen motor, it is not expected that machine windings should reach the maximum allowable temperature.

Experimental testing

In order to prove the previously established hypothesis, appropriate experimental testing was organized in the Laboratory for Hydraulic and Pneumatic Testing of the Faculty of Mechanical Engineering in Nis, Nis, Serbia.

Description of the experiment

The experiment was performed on a standard test rig (AMCA 210), with the suction duct with the diameter D = 690 mm (fig. 3) [6, 7]. Mechanical parameters that were measured were the differential pressure, Δp, and the rotational speed, n. The airflow of the fan was not measured in this study because it takes a long time, and it is also known from the theory of similarity of turbomachinery operation that the flow changes linearly with the change of rotational speed.

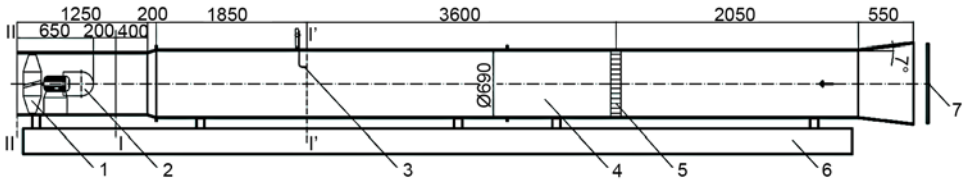

Figure 3. Test rig for the testing of axial flow fans; *1 – axial fan, 2 – deflector, 3 – Prandtl probe with traverse, 4 – testing channel, 5 – airflow straightener, 6 – stand, I′÷I′ – cross-section for measuring flow rate, I÷I – cross-section in front of the fan, II÷II – cross-section behind the fan*

Electric parameters of the induction motor (line voltage U, current I, active power P, and reactive power Q) were measured using a laboratory network analyzer, which was connected to a PC in order to enable efficient and fast recording of measured data. The wiring diagram of the equipment used in the experiment is shown in fig. 4, and it is important for better understanding the applied experimental procedure.

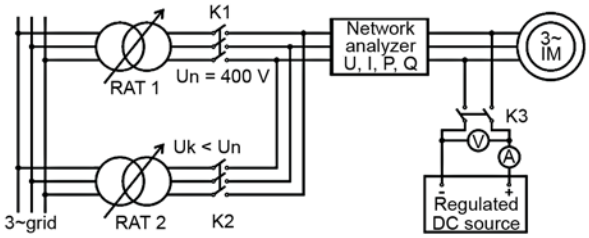

Figure 4. Wiring diagram of the electrical equipment used in the experiment

During the experimental testing, the ambient temperature in the Laboratory was $T_a = 292$ K, while the atmospheric pressure was $p_a = 991$ mbar. The experiment was organized in the following way:

At the very beginning, contactor K2 was closed (while K1 and K3 were opened) and the three phase voltage from the regulated autotransformer RAT2, that had been set to the value $U_k < U_n$, was applied to the stator windings of the induction machine, whose rotor was blocked. The value of U_k was chosen to obtain an approximately rated stator current $I_k \approx I_n$ flowing through the stator windings. Values of U_k , I_k and also consumed active power P_k and reactive power Q_k were recorded to the PC, connected with the laboratory network analyzer through the standard RS232 communication. Thus yielded results were accurately collected during a very short period (the reading lasted for only a few seconds), and in this way the unwanted temperature rise in the motor windings during the described impedance test was avoided. According to [1], an influence of the elements R_m and jX_m in the magnetizing branch of the equivalent circuit can be neglected during the impedance test performed with $U_k < U_n$, and thus, the sum of stator and rotor resistances can be calculated as:

$$R_k = R' + R_1'' = \frac{U_k}{\sqrt{3} I_k} \cdot \frac{P_k}{\sqrt{P_k^2 + Q_k^2}} \tag{4}$$

Immediately after the contactor K2 had been opened, the contactor K3 was closed and the voltage U_{DC} from the regulated DC source was applied to two of the three stator terminals. In this way, small current $I_{DC} \approx 0.4$ A was established through the serial connection of two phase windings (stator windings are in connected in Y), and based on the accurate reading of the applied voltage U_{DC} and the current I_{DC}, actual resistance of a stator per phase was calculated:

$$R' = \frac{U_{DC}}{2I_{DC}} \tag{5}$$

Using the values obtained from eqs. (4) and (5), the actual value of the rotor resistance per phase was calculated as $R_1'' = R_k - R'$.

Finally, after the contactor K3 had been opened, the contactor K1 was closed and the three-phase voltage $U = U_n = 400$ V was applied to the motor. As soon as the starting transient was finished, the measuring of time started, and the initial values of rotational speed n_{start} and total pressure Δp_{start} were recorded. The operation of the axial fan was continued for exactly 10 minutes, and during that period only slight corrections of voltage supplied to the motor were made, using the regulation autotransformer RAT1. This was done in order to eliminate the influence of voltage variations in the electric grid. During the preparation of the experimental testing, the impeller blade angle was set to the value that resulted in the highest possible value of the stator current $I \approx 3.45$ A, and the highest value of active power consumed from the electric grid was $P \approx 1750$ W. Thus, the almost nominal operating regime of the tested induction motor was achieved. At the end of the first 10-minute cycle of the motor operation, the rotational speed n and the total pressure Δp_{tot} were measured again, and immediately after, the contactor K1 was opened and the fan was stopped using a mechanical brake. The temperature of the motor housing T_{hous} [K] was then measured, using a non-contact laser thermometer, with the laser beam directed to the point located in the middle of the motor housing (the same point was always used for this type of measuring during the rest part of the experiment). At the same time, contactors K2 and K3 were used in the same way as in the beginning of the experiment, in order to perform the new impedance test and the new measuring of R'. After all of the described operations were completed (the imperative was to perform them very quickly to avoid the machine cooling), the contactor K1 was closed again and the next 10-minute cycle of operation started. The described procedure was repeated every 10 minutes. The experiment was stopped after 100 minutes, when it had become obvious that the motor operating point was not being changed anymore and that the steady-state values of rotational speed n_{steady} and Δp_{steady} were achieved. The test rig and the equipment used for experimental testing are shown in figs. 5 and 6.

Figure 5. The test rig

Figure 6. The electrical testing equipment

Measuring instruments

Characteristics of measuring instruments used for experimental testing are given in tabs. 1-6.

Table 1. Pressure

Instrument	Type	Accuracy	Range	Manufacturer
Manometer	MEDM 5K	±1% of v.reading	(0-5000) Pa	BSRIA

Table 2. Rotational speed

Instrument	Type	Accuracy	Range	Manufacturer
Tachometer	Digital	±0.04%±2	(1000-10000) rpm	Echtech

Table 3. Atmospheric pressure and temperature

Instrument	Type	Accuracy	Range	Manufacturer
Barometer	Manometer	1.0%	(890-1060) mbar	GDR
Thermometer	With mercury	0.5%	(0-50) °C	TGL

Table 4. Temperature of the motor housing

Instrument	Type	Accuracy	Range	Manufacturer
Thermometer	Infrared	1.0%	(0-200) °C	Raytek

Table 5. Electrical quantities

Instrument	Type	Accuracy	Range	Manufacturer
Laboratory network analyzer	AWM	±0.5% for U, I ±1.0% for P, Q	(5-265) V (line to neutral) (0-5)A (0-9999) MW (0-9999) MVAr (with current and voltage transformer)	ALFATEC
DC voltmeter	MTX 203	0.2% ± 2 dig	(0.6-5.999) V	METRIX
DC ampermeter	BL0120	0.5%	(0-0.6) A	ISKRA

Table 6. Data from the induction motor nameplate

manufacturer: SEVER	efficiency: η – given as diagram	rated voltage: U_n = 400 V
engine type: 1.7 KV 90 L-4	rated power: P = 1.5 kW	rated current: I_n = 3.6 A
serial number: 515281/06	rated power factor: cos φ_n = 0.79	number of phases: 3
rated speed: n = 1405 min^{-1}	rated frequency: f_n = 50 Hz	thermal tolerance class: F

Experimental results and discussion

Data related to electrical quantities measured during the experiment are presented in tab. 7.

Table 7. Measured electrical quantities

t [min]	U_k [V]	I_k [A]	P_k [W]	Q_k [VAr]	U_{DC} [V]	I_{DC} [A]
0	86.862	3.512	363.1	383.8	4.353	0.404
10	87.850	3.387	368.1	360.6	4.795	0.396
20	87.954	3.311	366.8	346.2	4.940	0.394
30	88.271	3.279	367.5	340.9	5.030	0.393
40	88.236	3.254	365.1	337.6	5.065	0.392
50	88.479	3.256	367.7	337.3	5.020	0.387
60	88.219	3.241	365.4	334.0	5.100	0.392
70	88.525	3.254	368.2	335.7	5.128	0.394
80	88.340	3.245	365.6	334.0	5.104	0.392
90	88.479	3.256	367.7	335.3	5.114	0.393
100	88.410	3.251	366.5	334.3	5.151	0.395

Based on data from tab. 7, using eqs. (5) and (4), the resistance of the stator winding R' and the resistance of the rotor winding R''_1 valid for different discrete times of the experiment were calculated in the first step of analysis. The second step was to calculate the actual mean temperature of the stator winding T_{stat} using eq. (2), and also the actual mean temperature of the rotor winding T_{rot} using eq. (3). Calculated results are presented in tab. 8, along with the results for directly measured quantities, temperature of the motor housing T_{hous}, rotational speed n and total pressure Δp_{tot}.

Table 8. Calculated resistances and temperatures of windings, and directly measured quantities

t [min]	Calculated using data from tab. 7				Directly measured		
	R' [Ω]	R_1'' [Ω]	T_{stat} [K]	T_{rot} [K]	T_{hous} [K]	n [min^{-1}]	Δp_{tot} [Pa]
0	5.387	4.426	292.000	292.000	292.00	1430.0	237.0
10	6.054	4.642	323.443	305.403	308.00	1425.6	236.0
20	6.269	4.884	333.568	320.331	313.50	1422.4	235.0
30	6.408	4.987	340.103	326.718	316.50	1419.8	234.0
40	6.460	5.033	342.593	329.587	319.50	1417.4	233.0
50	6.486	5.075	343.787	332.169	320.00	1416.7	232.5
60	6.505	5.096	344.698	333.493	320.50	1416.2	232.0
70	6.508	5.099	344.816	333.695	320.75	1416.0	232.0
80	6.510	5.093	344.938	333.324	320.75	1416.2	232.0
90	6.515	5.077	345.148	332.323	321.00	1416.1	232.0
100	6.520	5.080	345.412	332.484	321.25	1416.1	232.0

Calculated values of R' [Ω] and R''_1 [Ω] are presented in fig. 7.

Calculated values for the temperature in the stator windings T_{stat} [K] and the temperature in the rotor windings T_{rot} [K] are plotted in fig. 8, together with directly measured values for the temperature of the motor housing T_{hous} [K].

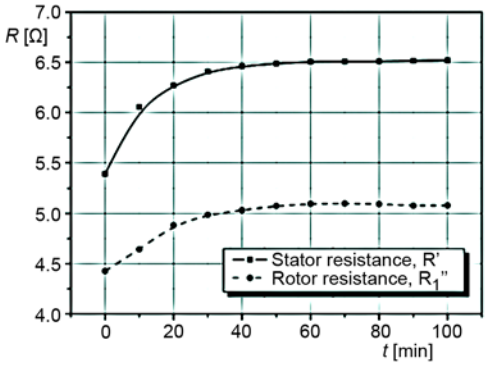

Figure 7. Variations of stator and rotor resistances during the experiment

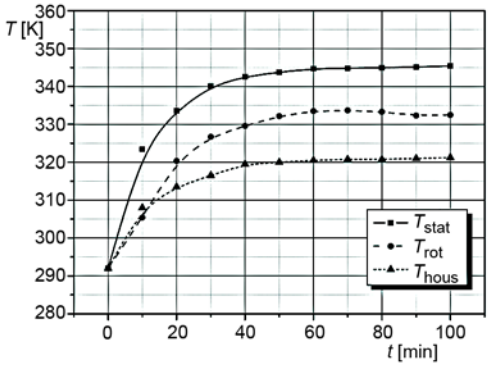

Figure 8. Temperature in the stator windings, temperature in the rotor windings, and temperature of the motor housing

From fig. 8 it is obvious that an induction motor must not be considered as thermally homogenous object, since different constructive parts of the machine show different temperature rises during the operation. The greatest temperature increase is detected in the stator windings, and that can be explained by the fact that most of power losses are concentrated in the stator segment of the machine. Besides losses caused by the current flow through the windings, power losses in the stator iron core also exist. The rotor part of the machine is affected only by power losses related to the current flow, while the iron core losses can be neglected due to very low frequency of the rotor magnetic flux in normal operation. It is also obvious that the temperature measured at the surface of the motor housing is always lower in the steady state operation, compared to the temperatures of stator and rotor windings.

Experimentally obtained results prove the assumption that such temperature rises cause significant increases in the motor windings resistance. Namely, the experiment showed that the resistance of the stator windings had risen from the initial value of $R'_{\text{start}} = 5.387\ \Omega$ to the steady-state value of $R'_{\text{steady}} = 6.520\ \Omega$, which gives $R'_{\text{steady}}/R'_{\text{start}} = 1.21$ (fig. 7.). At the same time, the resistance of the rotor windings had risen from the initial value of $R''_{1\text{start}} = 4.426\ \Omega$ to the steady-state value of $R''_{1\text{steady}} = 5.080\ \Omega$, *i. e.* $R''_{1\text{steady}}/R''_{1\text{start}} = 1.15$.

The detected rise of the temperature in the motor windings and the consequent rise of their resistances influence the shape of the motor torque-speed curve as supposed in section 2, and as the final consequence, a slight decrease in rotational speed can be observed from the start to the steady-state operation, as shown in fig. 9.

Observing the behavior of the system from the moment of the start of operation to the steady-state operation, one can conclude that the rotational speed was reduced by approximately 1% ($n_{\text{steady}}/n_{\text{start}} = 1.01$). In order to explain the shape of the experimentally obtained $n(t)$ curve, we have to analyze the way the stator and rotor resistances change, from the *cold* start to the *hot* steady-state operating

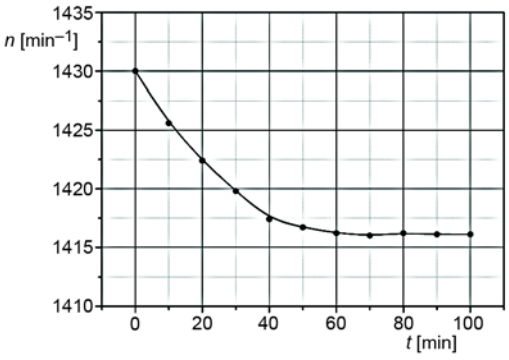

Figure 9. Variation of rotational speed during the experiment

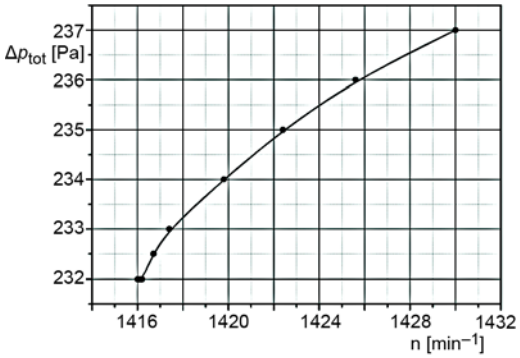

Figure 10. Variation of pressure with variation in rotational speed

regime. From fig. 8 it is obvious that the temperature rise is the most intense soon after the start of operation, while later on, when the temperature of the machine becomes significantly greater than the ambient temperature, the temperature rise slows down. The same pattern can be also observed in fig. 7, where resistances of motor windings have the greatest rise immediately after the start. This is in strong correlation with the observed fact that the rotational speed decreases at highest rates at the very beginning, while it decreases more slowly later. Figure 9 shows that the stable operating regime was achieved after 60 minutes.

The experiment confirmed that the pressure in the fan also varies with the variation in rotational speed, according to the square law $\Delta p_{start}/\Delta p_{steady} = (n_{start}/n_{steady})^2 = 1.02$, as shown in fig. 10.

Conclusions

The experimental testing whose results are shown in this paper clearly prove the hypothesis that the temperature rise in the induction motor windings causes a small reduction of the axial fan rotational speed, observing the period from the start of operation to the moment of achieving stationary operation. In the stationary regime, the rotational speed of the axial fan and the induction motor studied in the paper decreased for about 1%, while the total pressure decreased for about 2%, compared with the regime at the start. The reduction of rotational speed is the most intensive immediately after the start, because the temperature rise in the motor windings is very rapid in this period. After 60 minutes, the motor windings reached their stationary operating temperatures, while the rotational speed reached its steady-state value. This conclusion can not be generalized, since the induction motor with a low rated power was used in the experiment. In the case of a large motor with a significantly greater rated power, the period needed for reaching the steady-state operation could be several times longer. This information is very important primarily for accurate testing of the operating characteristics of a fan in laboratory conditions, but also for their practical application in certain sensitive types of industrial processes, that demand exact values of achieved volumetric flow and pressure.

In future investigations, the effects of an unbalanced supply voltage and the effects of a variable voltage on the variation in the rotational speed should be studied, in order to get a better understanding of the observed phenomenon.

Nomenclature

D – diameter, [m]
f – frequency, [Hz]
I – current, [A]
M – torque, [Nm]
n – actual rotor speed, [min^{-1}]
n' – synchronous speed, [min^{-1}]
P – power, [W]
p – pressure, [Pa]
Δp_{tot} – total pressure rise, [Pa]
Q – reactive power, [W]
R – resistance, [Ω]
R' – stator resistance per phase, [Ω]
R_1'' – rotor resistance per phase, [Ω]
s – relative slip [= $(n' - n)/n'$], [–]

T – temperature, [K]
U – voltage, [V]
U_f – RMS voltage per phase, [V]
X_m – magnetization reactance per phase, [Ω]
X'_γ – stator leakage reactance per phase, [Ω]
$X''_{\gamma k1}$ – rotor leakage reactance per phase, [Ω]

Greek symbols

Ω' – synchronous speed, [rad per second]
ν' – stator leakage factor (= $1 + X'_\gamma/X_m$), [–]

Subscripts

a – atmospheric, ambient
DC – direct current
k – indicating locked rotor variable
mot – motor
n – nominal
rot – rotor
stat – stator
tot – total

Acronyms

K – kontaktor
RAT – regulated autotransformer

References

[1] Stajić, Z., *et al.*, *Induction Machines* (in Serbian), Faculty of Electronic Engineering, Nis, Serbia, 2012
[2] Eck, B., *Fans-Design and Operation of Centrifugal, Axial-Flow, and Cross-Flow Fans*, Pergamon Press, Oxford, UK, 1973
[3] Spasić, Ž. T., *et al.*, Variation of Operation of Low-Pressure Reversible Axial Fans Driven by Induction Motor from Start to the Steady-State, *Proceedings*, 15th Symposium on Thermal Science and Engineering of Serbia, Sokobanja, Serbia, 2011, pp. 586-595
[4] Boldea, I., Nasar, S., *The Induction Machine Handbook*, CRC Press, New York, USA, 2002
[5] ***, IEC 60085 Electrical Insulation-Thermal Evaluation and Designation, International Electro-technical Commission, 4th ed., 2007
[6] Spasić, Ž. T., Numerical and Experimental Investigation of the Influence of the Blade Profile Shape on the Reversible Axial Fan Characteristics (in Serbian), Ph. D. thesis, University of Nis, Nis, Serbia, 2012
[7] Spasić, Ž. T., *et al.*, Low-Pressure Reversible Axial Fan with Straight Profile Blades and Relatively High Efficiency, *Thermal Science, 16* (2012), Suppl. 2, pp. S593-S603

Paper submitted: April 25, 2016
Paper revised: July 28, 2016
Paper accepted: September 21, 2016